BIOINFORMATICS ORIGINAL PAPER

Vol. 30 no. 6 2014, pages 808–814
doi:10.1093/bioinformatics/btt616

Gene expression

Advance Access publication October 27, 2013

# Direction pathway analysis of large-scale proteomics data reveals novel features of the insulin action pathway

Pengyi Yang[1,2,3,†], Ellis Patrick[2,†], Shi-Xiong Tan[3,4], Daniel J. Fazakerley[3], James Burchfield[3], Christopher Gribben[3], Matthew J. Prior[3], David E. James[3] and Yee Hwa Yang[2,*]

[1]Systems Biology Group, Biostatistics Branch, National Institute of Environmental Health Sciences, National Institute of Health, Research Triangle Park, NC 27709, USA, [2]School of Mathematics and Statistics, University of Sydney, [3]Diabetes and Obesity Program, Garvan Institute of Medical Research, NSW 2006, Australia and [4]Metabolism in Human Disease Unit, Institute of Molecular and Cellular Biology, A*Star, 61 Biopolis Drive, Proteos 138673, Singapore

Associate Editor: Janet Kelso

## ABSTRACT

**Motivation:** With the advancement of high-throughput techniques, large-scale profiling of biological systems with multiple experimental perturbations is becoming more prevalent. Pathway analysis incorporates prior biological knowledge to analyze genes/proteins in groups in a biological context. However, the hypotheses under investigation are often confined to a 1D space (i.e. up, down, either or mixed regulation). Here, we develop direction pathway analysis (DPA), which can be applied to test hypothesis in a high-dimensional space for identifying pathways that display distinct responses across multiple perturbations.

**Results:** Our DPA approach allows for the identification of pathways that display distinct responses across multiple perturbations. To demonstrate the utility and effectiveness, we evaluated DPA under various simulated scenarios and applied it to study insulin action in adipocytes. A major action of insulin in adipocytes is to regulate the movement of proteins from the interior to the cell surface membrane. Quantitative mass spectrometry-based proteomics was used to study this process on a large-scale. The combined dataset comprises four separate treatments. By applying DPA, we identified that several insulin responsive pathways in the plasma membrane trafficking are only partially dependent on the insulin-regulated kinase Akt. We subsequently validated our findings through targeted analysis of key proteins from these pathways using immunoblotting and live cell microscopy. Our results demonstrate that DPA can be applied to dissect pathway networks testing diverse hypotheses and integrating multiple experimental perturbations.

**Availability and implementation:** The R package '`directPA`' is distributed from CRAN under GNU General Public License (GPL)-3 and can be downloaded from: http://cran.r-project.org/web/packages/directPA/index.html

**Contact:** jean.yang@sydney.edu.au

**Supplementary Information:** Supplementary data are available at *Bioinformatics* online.

Received on April 11, 2013; revised on September 14, 2013; accepted on October 21, 2013

## 1 INTRODUCTION

Pathway analysis has become a key approach to incorporate prior knowledge for interpreting '-omics' scaled data generated from high-throughput techniques such as microarray, RNA-seq and quantitative mass spectrometry (MS)-based proteomics. It has the advantage of leveraging high dimensionality and limited replicates by organizing genes and proteins into groups and analyzing them in biological meaningful contexts (Nam and Kim, 2008).

To date, numerous pathway analysis approaches have been proposed (Emmert-Streib and Glazko, 2011) and several taxonomies have been described to categorize them (Ackermann and Strimmer, 2009; Goeman and Bühlmann, 2007; Huang *et al.*, 2009; Irizarry *et al.*, 2009). One of the popular categorization approaches is to classify pathway analysis methods as using an *over-representation* approach or *aggregate score* approach (Irizarry *et al.*, 2009). The over-representation approach, exemplified by hypergeometric test using Gene Ontology (GO) (Khatri and Drăghici, 2005; Rivals *et al.*, 2007), requires a preselected list of differentially expressed (DE) genes to be supplied before the test. It could be sensitive to the cut-off applied to select DE genes (Irizarry *et al.*, 2009). The aggregate score approach, exemplified by gene set enrichment analysis (GSEA) (Mootha *et al.*, 2003; Subramanian *et al.*, 2005), alleviates this requirement by considering statistics associated with all genes for testing pathway differential regulation.

There are several recent extensions on pathway analysis. These include the extensions from univariate to multivariate statistics such as the use of Hotelling's $T^2$-statistics and N-statistics (Klebanov *et al.*, 2007; Kong *et al.*, 2006) and from single analysis to meta-analysis such as combining results from multiple studies (Shen and Tseng, 2010), different platforms (Poisson *et al.*, 2011) and/or multiple methods (Väremo *et al.*, 2013). Nevertheless, current pathway analysis methodologies are mainly designed for testing hypotheses in a 1D space and focus on identifying pathways that show up, down, either or mixed differential regulations. Due to the growing complexity of large-scale experiments where multiple treatments are applied, for example, to dissect the signalling networks, a novel pathway analysis approach that can incorporate multiple perturbations into a single statistical analysis is desirable.

*To whom correspondence should be addressed
†The authors wish it to be known that, in their opinion, the first two authors should be regarded as joint First Authors.

The broad term *experimental perturbations* is used to describe any situation in which a cell has been agitated and its reaction quantified. Practically speaking when referring to multiple experimental perturbations, we may be referring to quantifying the effects of a treatment versus control at various cellular levels (DNA, RNA, protein). We could also consider multiple experimental perturbations to refer to various treatment comparisons at the same cellular level.

In this study, we propose *direction pathway analysis* (DPA) for integrating multiple perturbations in pathway analysis. This method integrates multiple experimental perturbations by coupling coordinate rotation with *P*-value combination techniques. It extends on traditional pathway analysis in the following aspects:

- The method increases statistical power by integrating multiple perturbations for testing in a high-dimensional space.
- The method improves biological interpretability by translating a biological question into a direction-specific test, broadening the hypothesis space and allowing many more biological questions to be investigated.
- The method is flexible and can be extended to *n*-dimensions, where *n* is the number of experimental perturbations.

To demonstrate the effectiveness of *P*-value combination techniques at answering various alternative hypotheses, we designed and performed a set of simulation studies. These studies offer insight into the selection of an appropriate combination technique for DPA in integrating information on testing pathway enrichment.

To explore the utility of the method, we applied this approach to MS-based proteomics data obtained from adipocytes aiming to identify insulin action pathways under various treatments. Adipocytes are one of the major targets of insulin action in mammals. One of the major pathways downstream of the insulin receptor is the phosphatidylinositol-3-kinase (PI3K)-Akt pathway (Engelman *et al.*, 2006; Manning and Cantley, 2007). To date, the majority of evidence points towards Akt alone being sufficient to elicit the majority of insulin's intracellular actions (Ng *et al.*, 2008). However, there are PI3K-dependent Akt-independent pathways that are activated by insulin stimulation (Choi *et al.*, 2010) and it is possible that such pathways may also regulate protein trafficking events in response to insulin. To dissect PI3K-Akt pathways and determine the contributions of Akt-independent and Akt-dependent pathways, we used various pharmacological agents to target different signal transduction nodes and subsequently performed plasma membrane purification and SILAC-based (Ong *et al.*, 2002) quantitative proteomic profiling (Ong and Mann, 2005). By analyzing the proteomic profile using DPA, we identified that several pathways were enriched in the plasma membrane following insulin stimulation, and that these trafficking events were strongly dependent on PI3K signalling. However, the translocation of these pathways was not fully blocked in the presence of an Akt inhibitor, suggesting that there are Akt-independent pathways that promote membrane trafficking events in response to insulin. We validated these findings through targeted analysis of several key proteins from these insulin-regulated pathways using immunoblotting and live cell microscopy.

## 2 MATERIALS AND METHODS

### 2.1 Direction pathway analysis

In this study, we propose a novel approach, called DPA, for a direction-specific pathway test (Fig. 1). Our approach consists of three main steps:

(1) Rotating a matrix of test statistics such that large values of the test statistics provide evidence against the null hypothesis in favour of the alternative;

(2) Combining the statistics across multiple experimental perturbations for each protein using a *P*-value combination method; and

(3) Combining the statistics across proteins within a pathway using a *P*-value combination method.

The novelty of this approach is the concept of *P*-value rotation for testing pathways in a specific direction and the tandem application of *P*-value combination methods for integrating information across multiple experimental perturbations of each protein (protein level integration) and multiple proteins within a pathway (pathway level integration).

*2.1.1 P-value combination* There are many methodologies for combining information across studies or within pathways and the key discriminating differences between many of these methods are their assumed alternative hypotheses (Tseng *et al.*, 2012). Let $\tau_j$ represent test statistics for $j = 1, 2, \ldots, n$, where $n$ are the number of tests. Assume the null hypothesis that none features measured by these test statistics have changed ($H_0 : \tau_j = 0,\ \forall\, j = 1, 2, \ldots, n$). Li and Tseng (2011) proposed to classify different alternative hypotheses into two broad classes $H_A$ and $H_B$. Alternative hypothesis $H_A$ is used to detect a series of tests in which *all* the tests have changed ($H_A : \tau_j > 0,\ \forall\, j = 1, 2, \ldots, n$). Alternative hypothesis $H_B$ is used to detect a series of tests in which *any* of the tests have changed ($H_B : \tau_j > 0,$ for at least one $j$ in $1, 2, \ldots, n$).

For our DPA, we would like to identify pathways that have had *any* of their proteins changed in *all* experimental perturbations in the direction of interest. When put in the context of *P*-value combination, this would then require the tandem use of combination methods that favourable to testing $H_0$ against $H_A$ when combining across experimental perturbations and $H_0$ against $H_B$ when combining within a pathway, respectively.

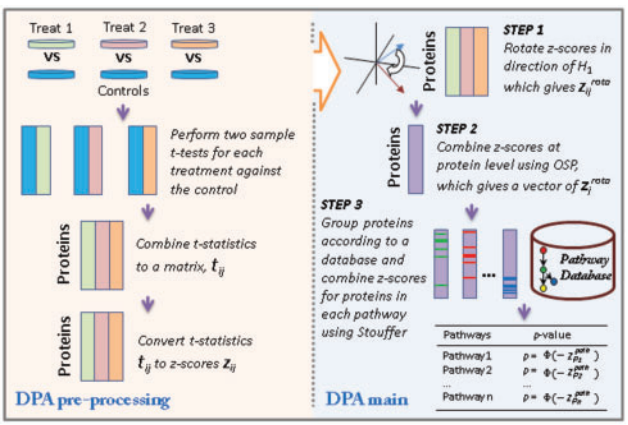


**Fig. 1.** The workflow of DPA. The DPA pre-processing panel summarizes the combination and generation of a *z*-score matrix from multiple experimental perturbations. The DPA main panel summarizes the application of the rotation and integration steps to test for pathway significance

In our proposed DPA approach, we utilize Stouffer's method (Stouffer *et al.*, 1949) to combine within pathways. This is defined as

$$\textbf{Stouffer}: \Phi\left(\frac{1}{n}\sum_{j=1}^{n}\Phi^{-1}(p_j)\right),$$

where $\Phi(.)$ is the cumulative distribution function for the standard normal distribution and for independent $P$-values $p_j$, $j = 1, \ldots, n$. To combine across experimental perturbations, we will use a one-sided version of Pearson's method (Pearson, 1934), OSP, defined as

$$\textbf{OSP}: \mathrm{P}\left(\chi^2_{2n} < -2\sum_{j=1}^{n}\log(1-p_j)\right).$$

This method is not that proposed by Pearson (1934) but is mentioned in later work (Pearson, 1938).

The combined $P$-values for Stouffer converge to zero if any one of the $p_j$ also converges to zero making it appropriate for testing $H_0$ against the alternative $H_B$. For OSP to converge to zero, all $p_j$ must converge to zero, thus making it appropriate for testing $H_0$ against the alternative $H_A$. To demonstrate the behaviour of the $P$-value combination methods and justify the selection of appropriate ones for our application, further explanation and a set of simulation studies were performed (see Section 1 of Supplementary File).

*2.1.2 Rotation and combination* Our DPA takes as input three vectors of test statistics. The left panel of Figure 1 describes how these statistics may be generated and processed before performing the three main steps of DPA (the right panel of Fig. 1). This process is described more formally as follows. Define a matrix of test statistics $\tau$, where $\tau_{ij}$ is the test statistic for the $i^{th}$ protein, $i = 1, 2, \ldots, n_p$, in one of three experimental perturbations, $j = 1, 2, 3$. Let $t_{ij}$ correspond to the observed $\tau_{ij}$. These test statistics have most likely come from multiple two-sample $t$-tests but could be other statistics such as regression coefficients. We assume that a subset of these proteins belong to pathway $\mathcal{P}$, and that the $\tau_{ij}$ are independent, which may not be the case in practice. The test statistics $\tau_{ij}$ may not be identically distributed. They can be converted into identically distributed $z$-scores, $z_{ij}$, which are easier to manipulate by first evaluating their corresponding one-sided probabilities $p_{ij} = \mathrm{P}(\tau_{ij} > t_{ij})$. The matrix of $z$-scores are then defined as $z_{ij} = -\Phi^{-1}(p_{ij})$, where $\mathrm{P}(\tau_{ij} > t_{ij}) = \mathrm{P}(\zeta_{ij} > z_{ij})$.

DPA tests if any of the proteins in pathway $\mathcal{P}$ have deviated from the null hypothesis in the direction of the alternative hypothesis. A specific example may be written as

$$\begin{cases} H_0: & \tau_{i1} = 0, \tau_{i2} = 0, \tau_{i3} = 0; \text{for all } i \in \mathcal{P} \\ H_1: & \tau_{i1} > 0, \tau_{i2} < 0, \tau_{i3} = 0; \text{for any } i \in \mathcal{P}, \end{cases} \quad (1)$$

testing if any proteins in pathway $\mathcal{P}$ have been upregulated in the first perturbation, downregulated in the second perturbation and remain unchanged in the third perturbation. The three steps of rotation, combination at protein level and combination at pathway level are outlined in the right panel of Figure 1 and described in more detail in the following:

**Step 1.** The matrix $\mathbf{z}$ is rotated such that large values within $\mathbf{z}$ provide evidence against the null hypothesis in favour of the alternative hypothesis. This is achieved as follows:

(a) Represent the direction of the alternative hypothesis using the unit vector $\mathbf{v} = (v_1, v_2, v_3)$ where each element corresponds to the direction of interest in the experimental perturbation. If considering the example test described in Equation (1) then $\mathbf{v}$ would be defined as $\mathbf{v} = (1/\sqrt{2}, -1/\sqrt{2}, 0)$.

(b) Represent the direction that we would like to rotate to as $\mathbf{u} = (u_1, u_2, u_3) = (1/\sqrt{3}, 1/\sqrt{3}, 1/\sqrt{3})$ and calculate the angle between $\mathbf{u}$ and $\mathbf{v}$ as $\theta = \cos^{-1}(\mathbf{u}\cdot\mathbf{v}) = \cos^{-1}(u_1v_1 + u_2v_2 + u_3v_3)$.

(c) Let $\mathbf{a} = \mathbf{u} \times \mathbf{v} = (u_2v_3 - u_3v_2, u_3v_1 - u_1v_3, u_1v_2 - u_2v_1)$, which is a vector that is orthogonal to $\mathbf{u}$ and $\mathbf{v}$.

(d) We can then define $\mathbf{R}$ as the matrix for a clockwise rotation around the vector $\mathbf{a}$ by an angle of $\theta$ as

$$\mathbf{R} = \mathbf{I} + \sin\theta \begin{bmatrix} 0, -a_3, a_2 \\ a_3, 0, -a_1 \\ -a_2, a_1, 0 \end{bmatrix} + (1-\cos\theta) \begin{bmatrix} a_1^2 - 1, a_1a_2, a_1a_3 \\ a_1a_2, a_2^2 - 1, a_2a_3 \\ a_1a_3, a_2a_3, a_3^2 - 1 \end{bmatrix}. \quad (2)$$

(e) We define $\mathbf{z}^{rota} = \mathbf{z}\mathbf{R}^{\mathbf{T}}$ as the rotated $z$-scores.

**Step 2.** Now that the $z$-scores are orientated in the direction of interest, they can be combined across experimental perturbations to provide evidence that each protein is DE in the direction described by the alternative hypothesis $H_1$. The rotated $z$-scores are combined using OSP for each protein to form the vectors $\mathbf{p}^{prot}$ and $\mathbf{z}^{prot}$ as follows:

$$p_i^{prot} = \mathrm{P}\left(\chi^2_6 < -2\sum_{j=1}^{3}\log\left(1 - \Phi(-z_{ij}^{rota})\right)\right). \quad (3)$$

These protein significance values can then be converted back to $z$-scores by evaluating this combined $P$-value with respect to the upper tail of the normal distribution

$$z_i^{prot} = -\Phi^{-1}(p_i^{prot}). \quad (4)$$

**Step 3.** We can then test if a pathway $\mathcal{P}$ is differentially regulated in the direction described by the alternative hypothesis $H_1$ using Stouffer's method. The $z$-scores can be combined for each pathway as follows:

$$z_{\mathcal{P}}^{path} = \frac{\sum_{i=1}^{n_p} z_i^{prot} 1\{i \in \mathcal{P}\}}{\sqrt{\sum_{i=1}^{n_p} 1\{i \in \mathcal{P}\}}}. \quad (5)$$

Significance can be calculated for each pathway by evaluating this combined $z$-score with respect to the upper tail of the normal distribution

$$p_{\mathcal{P}}^{path} = \Phi(-z_{\mathcal{P}}^{path}). \quad (6)$$

## 2.2 Methods for quantifying insulin action in plasma membrane trafficking

We collected data generated from our previous study (Prior *et al.*, 2011) and performed new proteomic profiling experiment in this study with additional treatments (Fig. 2). In the previous experiment, cultured 3T3-L1 fibroblasts were left unlabelled ('light'), SILAC labelled with $^{13}C_6$-arginine and $^{2}H_4$-lysine ('medium') or $^{13}C_6$-$^{15}N_4$-arginine and $^{13}C_6$-$^{15}N_2$-lysine ('heavy'). The cells cultured with $^{13}C_6$-arginine and $^{2}H_4$-lysine were stimulated with 100 nM insulin for 20 min and the cells cultured with $^{13}C_6$-$^{15}N_4$-arginine and $^{13}C_6$-$^{15}N_2$-lysine were treated with 100 nM wortmannin, a PI3K inhibitor, for 20 min before insulin stimulation. The unlabelled cell culture was left unstimulated to establish basal condition. In this study, a second set of plasma membrane proteomic profiling experiments were performed with a similar procedure as described earlier in text except that the 'light' cells were treated with 10 uM MK-2206, an Akt inhibitor (Tan *et al.*, 2011), for 30 min before the stimulation of insulin (100 nM) for 20 min, 'Medium' cells were left unstimulated as basal condition and 'Heavy' cells were treated with 0.1% DMSO for 30 min before the addition of 100 nM insulin for 20 min. After establishing multiple treatments, cell lysates were mixed with ratio 1:1:1 in both sets of experiments, and subcellular fractionation were performed to enrich plasma membrane fraction. MS-based profiling was conducted using a LTQ-FT Ultra mass spectrometer and an Orbitrap Velos mass spectrometer (Thermo Fisher Scientific). The combined dataset was quantified using MaxQuant (Cox and Mann, 2008) and 997 proteins were quantified in all treatments.

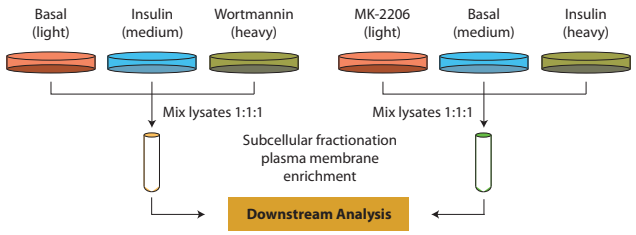


**Fig. 2.** MS-based plasma membrane proteomic profiling and analysis. Two sets of SILAC-based quantitative proteomics were performed to quantify plasma membrane proteome level in basal condition, insulin stimulation, prior inhibition of PI3K using Wortmannin followed by insulin stimulation and prior inhibition of Akt using MK-2206 followed by insulin stimulation

For DPA analysis validation, key proteins prioritized by DPA were selected for immunoblotting and live cell microscopy. The extended experimental procedures can be found in Section 2 of Supplementary File.

## 3 RESULTS

### 3.1 Direction pathway analysis on insulin action in plasma membrane proteome trafficking

The PI3K-Akt pathway serves as a crucial channel for insulin-regulated processes in adipocytes. This pathway contains two key nodes; the lipid kinase PI3K (Engelman *et al.*, 2006) and the protein kinase Akt (Manning and Cantley, 2007). Akt has been reported to phosphorylate numerous substrates to elicit the control over the numerous cellular processes regulated by insulin. While much of insulin's actions are attributed to the combined action of the PI3K/Akt axis, little work has been done to establish the role of PI3K and/or Akt independent pathways in these processes.

DPA could be applied as an exploratory tool for dissecting the relative requirement for PI3K and Akt in the insulin response in pathways associated with plasma membrane proteome. To this end, we performed large-scale plasma membrane proteome quantification using a quantitative MS-based protoemics approach with SILAC labelling and subcellular fractionation. The PI3K and Akt nodes were pharmacologically inhibited using wortmannin (Arcaro and Wymann, 1993) or MK-2206 (Tan *et al.*, 2011), respectively, before insulin stimulation, and the protein abundance on the cell plasma membrane were quantified according to the peak intensity from SILAC label. Let the test statistics $\tau_{i1}$, $\tau_{i2}$ and $\tau_{i3}$ represent the comparisons of basal condition to the treatment of (i) insulin alone; (ii) wortmannin before insulin; and (iii) MK-2206 before insulin, respectively, for the $i^{th}$ protein. With these panels of perturbations, we are interested in testing the following three scenarios described by Tests 1, 2 and 3:

- **Test 1.** A pathway $\mathcal{P}$ enriched within the plasma membrane after insulin stimulation ('>') and this enrichment is reduced to a negative level by prior inhibition of PI3K ('<') but remain unaffected by Akt. These are PI3K-dependent, Akt-independent events.

$$\begin{cases} H_0: & \tau_{i1}=0, \tau_{i2}=0, \tau_{i3}=0; \text{for all } i\in\mathcal{P} \\ H_1: & \tau_{i1}>0, \tau_{i2}<0, \tau_{i3}>0; \text{for any } i\in\mathcal{P}, \end{cases} \quad (7)$$

with $\mathbf{v}=\left(\frac{1}{\sqrt{3}},\frac{-1}{\sqrt{3}},\frac{1}{\sqrt{3}}\right)$ and $\mathbf{u}=\left(\frac{1}{\sqrt{3}},\frac{1}{\sqrt{3}},\frac{1}{\sqrt{3}}\right)$.

- **Test 2.** A pathway $\mathcal{P}$ enriched within the plasma membrane after insulin stimulation and this enrichment is reduced to a negative level by prior inhibition of PI3K but only to the unstimulated level by Akt ('='). These are PI3K-dependent, partially Akt-dependent events.

$$\begin{cases} H_0: & \tau_{i1}=0, \tau_{i2}=0, \tau_{i3}=0; \text{for all } i\in\mathcal{P} \\ H_1: & \tau_{i1}>0, \tau_{i2}<0, \tau_{i3}=0; \text{for any } i\in\mathcal{P}, \end{cases} \quad (8)$$

with $\mathbf{v}=\left(\frac{1}{\sqrt{2}},\frac{-1}{\sqrt{2}},0\right)$ and $\mathbf{u}=\left(\frac{1}{\sqrt{3}},\frac{1}{\sqrt{3}},\frac{1}{\sqrt{3}}\right)$.

- **Test 3.** A pathway $\mathcal{P}$ enriched within the plasma membrane after insulin stimulation and this enrichment is reduced to a negative level by prior inhibition of PI3K or Akt. These are PI3K-dependent, Akt-dependent events.

$$\begin{cases} H_0: & \tau_{i1}=0, \tau_{i2}=0, \tau_{i3}=0; \text{for all } i\in\mathcal{P} \\ H_1: & \tau_{i1}>0, \tau_{i2}<0, \tau_{i3}<0; \text{for any } i\in\mathcal{P}, \end{cases} \quad (9)$$

with $\mathbf{v}=\left(\frac{1}{\sqrt{3}},\frac{-1}{\sqrt{3}},\frac{-1}{\sqrt{3}}\right)$ and $\mathbf{u}=\left(\frac{1}{\sqrt{3}},\frac{1}{\sqrt{3}},\frac{1}{\sqrt{3}}\right)$.

Note that by 'reduced to a negative level' we mean the inhibition not only blocks the insulin simulation but also removes any residual insulin effect compared with the unstimulated condition. Therefore, this effect is denoted as '<'. The hypotheses under testing in the aforementioned three scenarios are visualized in Figure 3.

At the individual protein level, DPA prioritizes proteins based on the $z$-score calculated from OSP across conditions (Fig. 3). The most significant proteins from the tests are coloured in red, whereas the least significant ones are in purple. The top ranked proteins are listed under the panel of each tested directions (Fig. 3). These proteins include Syntaxins (Syntaxin-6, Syntaxin-7, Syntaxin-8 and Syntaxin-12) and vesicle-associated membrane proteins (VAMP2, VAMP3 and VAMP8) from the family of SNARE proteins, as well as several other proteins known to localize with intracellular glucose transporter vesicles including GLUT4 itself and the transferrin receptor (TfR). Also highly ranked are the lipid phosphate phosphohydrolase 2 (PPAP2A) and lipid phosphate phosphohydrolase 3 (PPAP2B), which regulate the glycerolipid synthesis and have been reported to be involved in signal transduction at the plasma membrane (Nanjundan and Possmayer, 2001).

Interestingly, many pathways associated with vesicle trafficking and lipolysis are highly enriched described by Test 2 (Table 1). These include *Proteolytic cleavage of SNARE complex proteins*, *clathrin derived vesicle budding*, *golgi associated vesicle biogenesis*, *membrane trafficking* and *lysosome vesicle biogenesis* which are primarily associated with insulin-dependent glucose transport, the primary action of insulin in adipocytes. Two pathways, *Sphingolipid metabolism* and *Triglyceride biosynthesis*, are associated with lipolysis, a process that is also known to be regulated by the PI3K-Akt pathway in response to insulin stimulation. These results indicate that protein molecules from these pathways are enriched within the plasma membrane with insulin stimulation, and while the inhibition of PI3K using wortmannin significantly abolished their enrichment, the inhibition of Akt using MK-2206 only had a partial effect. This implies that while insulin actions are largely dependent on the canonical activation of PI3K and Akt, there may exist a PI3K-dependent, but Akt-independent branch of the insulin signalling that plays a significant but less

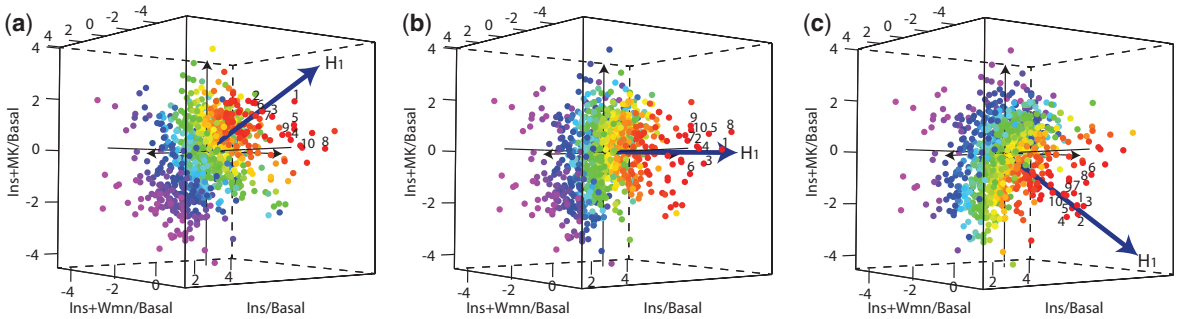


| ID | Protein Name |
|---|---|
| 1 | STEAP4 (Metalloreductase STEAP4) |
| 2 | EIF4G1 (Eukaryotic translation initiation factor 4) |
| 3 | COL15A1 (Collagen alpha-1(XV) chain) |
| 4 | M6PR (Mannose 6-phosphate receptor) |
| 5 | TfR (Transferrin receptor) |
| 6 | ILVBL(Acetolactate synthase-like protein) |
| 7 | STEAP3 (Metalloreductase STEAP3) |
| 8 | PPAP2A (Lipid phosphate phosphohydrolase 1) |
| 9 | GLUT4 (Glucose transporter type 4) |
| 10 | DNAJC13 (DnaJ homolog subfamily C member 13) |

| ID | Protein Name |
|---|---|
| 1 | PPAP2A (Lipid phosphate phosphohydrolase 1) |
| 2 | SYPL1 (Synaptophysin-like protein 1) |
| 3 | VAMP3 (Vesicle-associated membrane protein 3) |
| 4 | DNAJC13 (DnaJ homolog subfamily C member 13) |
| 5 | STX6 (Syntaxin 6) |
| 6 | VAMP2 (Vesicle-associated membrane protein 2) |
| 7 | M6PR (Mannose 6-phosphate receptor) |
| 8 | BASP1 (Brain acid soluble protein 1) |
| 9 | GLUT4 (Glucose transporter type 4) |
| 10 | TfR (Transferrin receptor) |

| ID | Protein Name |
|---|---|
| 1 | VAMP8 (Vesicle-associated membrane protein 8) |
| 2 | STX7 (Syntaxin 7) |
| 3 | VTI1B (Vesicle transport with t-SNAREs homolog 1B) |
| 4 | ATP6V0A1 (V-type proton ATPase 116 kDa subunit a1) |
| 5 | STX8 (Syntaxin 8) |
| 6 | VAMP2 (Vesicle-associated membrane protein 2) |
| 7 | SCAMP3 (Secretory carrier-associated membrane protein 3) |
| 8 | STX12 (Syntaxin 12) |
| 9 | NCSTN (Nicastrin) |
| 10 | ANXA1 (Annexin A1) |

**Fig. 3.** Projections of plasma membrane proteome using DPA. A total of 997 proteins with quantitation in all treatments are coloured by their statistical significance calculated from OSP across perturbations on the tested directions. The red proteins are the most significant and purple are the least significant proteins. Plots (**a–c**) are the scatter plots of plasma membrane proteome from testing in the directions described by tests 1, 2 and 3, respectively. The top-10 proteins ranked on each direction are further listed below the scatter plots

**Table 1.** Significant pathways from Test 2 in insulin stimulated plasma membrane trafficking in adipocytes

| Pathway | Size | Probability | Rank | Associated functions |
|---|---|---|---|---|
| Proteolytic cleavage of SNARE complex proteins | 7 | $2 \times 10^{-9}$ | 1 | Traffic and transport |
| Clathrin derived vesicle budding | 17 | $2 \times 10^{-6}$ | 2 | Traffic and transport |
| Golgi associated vesicle biogenesis | 15 | $2 \times 10^{-5}$ | 3 | Traffic and transport |
| Sphingolipid metabolism | 7 | $2 \times 10^{-4}$ | 4 | Lipolysis |
| Membrane trafficking | 21 | $6 \times 10^{-4}$ | 5 | Traffic and transport |
| Lysosome vesicle biogenesis | 9 | 0.003 | 6 | Traffic and transport |
| Triglyceride biosynthesis | 7 | 0.034 | 10 | Lipolysis |

*Note:* The size column indicates the number of identified and quantified proteins of a given pathway, and the rank column shows the rank of each pathway.

dominant role in insulin-regulated protein trafficking. The complete list of pathways analysis results on the three tested directions is included in the Supplementary Table.

To experimentally validate the PI3K-dependent and partial Akt-dependent effect suggested by PDA analysis of plasma membrane proteome, several key proteins from these enriched pathways were selected for immunoblotting and live cell imaging.

## 3.2 Validating PI3K-dependent and partial Akt-dependent regulations

Using DPA, we discovered that many pathways associated with vesicle trafficking and glucose translocation in adipocytes are regulated by insulin in a PI3K-dependent and partially Akt-dependent manner. Here, we select several key proteins from these pathways to validate the results from DPA analysis.

*3.2.1 Immunoblotting of trafficking proteins* Immunoblotting analysis demonstrated that the cytosolic protein tubulin was absent from the plasma membrane fraction, whereas a known plasma membrane protein cadherin was highly enriched (Fig. 4b). This confirms that the plasma membrane isolation method resulted in a pure membrane fraction. Compared with the loading control of 14-3-3, insulin treatment led to increased phosphorylation of Akt at pThr308 and its downstream substrates pThr642 AS160 and pSer246 PRAS40 (Fig. 4a). Pretreatment of cells with either the PI3K inhibitor wortmannin or the Akt inhibitor MK-2206 completely abolished Akt phosphorylation and its activity as demonstrated by complete diminution of substrate phosphorylation (Fig. 4a). These data indicate that these inhibitors completely block PI3K or Akt activity.

To validate our observation from DPA results that many insulin-responsive trafficking events are PI3K-dependent, but partial Akt-dependent (Fig. 3), we chose two key vesicle trafficking proteins, Syntaxin-6 and VAMP2, for immunoblotting. Syntaxin-6 and VAMP2 are members of the SNARE family of proteins and are known to regulate GLUT4 trafficking in 3T3-L1 adipocytes (Perera *et al.*, 2003; Zhao *et al.*, 2009). As expected, insulin treatment increased plasma membrane levels

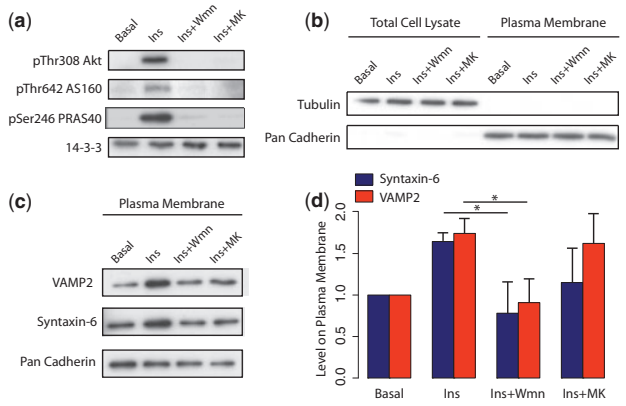


**Fig. 4.** Immunoblotting of vesicle trafficking proteins. (**a**) Insulin stimulation and inhibitor efficacy control panel. (**b**) Plasma membrane isolation control panel. (**c**) Immunoblotting of Syntaxin-6 and VAMP2 proteins in plasma membrane fraction. (**d**) Bar graph represents densitometry quantification of the immunoblots normalized to that of cadherin. The entire experiments were repeated three times and the error bars represent the standard deviations in three experiments. $^{*}P<0.05$

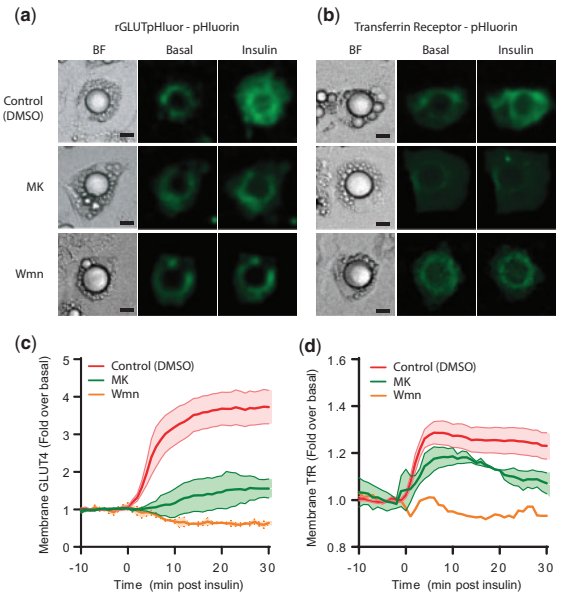


**Fig. 5.** Microscopy of GLUT4 and TfR. (**a** and **b**) are images of 3T3-L1 adipocytes expressing either (a) rGLUTpHluor or (b) TfR-pH pre-treated with either DMSO (control), wortmannin, of MK-2206 before the insulin stimulation. Individual cells are shown before and 20 min after stimulation with insulin. Scale bar equals to 10 $\mu$m. (**c** and **d**). Time course of insulin stimulated changes in the PM levels of (c) GLUT4 and (d) TfR-pH pre-treated with either MK-2206, wortmannin or DMSO (control). Data represent the mean ± standard error from 3–5 experiments

of both Syntaxin-6 and VAMP2, and wortmannin treatment abolished the effect of insulin (Fig. 4c and d). In agreement with the DPA results from proteomics experiments, Syntaxin-6 and VAMP2 had higher levels at the plasma membrane when treated with the MK-2206 compared with wortmannin (Fig. 4c and d).

*3.2.2 Live cell microscopy of transporter proteins* We next sought to further validate this phenomenon by using live cell microscopy. In adipocytes, one of the most physiologically important insulin responsive trafficking events is the translocation of the insulin-responsive glucose transporter type 4 (GLUT4) to the plasma membrane. The TfR has also been reported to traffick to the plasma membrane in an insulin-responsive manner. Both of two proteins ranked highly in our DPA results (Fig. 3a and b). Given an incomplete inhibition of the SNARE protein trafficking (e.g. Syntaxin-6 and VAMP2) to the plasma membrane in the presence of MK-2206, we next determined whether this pattern also held true for GLUT4 and TfR translocation events. We made use of a dual colour GLUT4 construct and TfR constructs (Burchfield *et al.*, 2012) as read outs for GLUT4 and TfR translocation, respectively.

In the time course live cell microscopy experiment, insulin robustly increased GLUT4 and TfR plasma membrane levels (Fig. 5). Wortmannin completely inhibited insulin mediated GLUT4 translocation to the plasma membrane, whereas MK-2206 exhibited only partial inhibition (Fig. 5c). A similar trend was also observed for TfR translocation to the plasma membrane (Fig. 5d).

## 4 CONCLUSION

In this study, we developed DPA for detecting biologically relevant pathways under multiple experimental perturbations. This method tests a hypothesis by rotating the test statistics and combining across both proteins and multiple experimental perturbations using *P*-value combination. Compared with traditional pathway analysis, DPA allows many more biological questions formulated as an alternative hypothesis and tested directly. We subsequently applied DPA to identify pathways that are significantly enriched at the plasma membrane in response to insulin stimulation and differentially inhibited by different inhibitors with the goal of dissecting insulin-regulated processes and their dependence on PI3K and Akt kinases. By examining a specific alternative hypothesis, we identified several key regulatory pathways to be plasma membrane enriched in a PI3K-dependent and partial Akt-dependent way. We then validated the key proteins in these pathways using immunoblotting and live cell microscopy techniques. Collectively, this study demonstrates the usefulness of the proposed DPA approach to aid the analysis of global datasets generated from experiments consisting of multiple perturbations. In this case, DPA helped identify and dissect the key signalling nodes of insulin regulation in adipocytes.

*Funding*: Australian Research Council (ARC) grants (FT0991918 and DP0984267 to Y.Y.) and by an National Health and Medical Research Council (NHMRC) program grant (to D.E.J.). D.E.J. is also recipient of an NHMRC Senior Principal Research. D.F. is a Sir Henry Wellcome Post-Doctoral Fellow of the Wellcome Trust.

*Conflict of Interest:* none declared.

## REFERENCES

Ackermann,M. and Strimmer,K. (2009) A general modular framework for gene set enrichment analysis. *BMC Bioinformatics*, **10**, 47.

Arcaro,A. and Wymann,M. (1993) Wortmannin is a potent phosphatidylinositol 3-kinase inhibitor: the role of phosphatidylinositol 3, 4, 5-trisphosphate in neutrophil responses. *Biochem. J.*, **296** (Pt. 2), 297.

Burchfield,J. *et al.* (2012) Novel systems for dynamically assessing insulin action in live cells reveals heterogeneity in the insulin response. *Traffic*, **14**, 259–273.

Choi,S.M. *et al.* (2010) Insulin regulates adipocyte lipolysis via an akt-independent signaling pathway. *Mol. Cell. Biol.*, **30**, 5009–5020.

Cox,J. and Mann,M. (2008) Maxquant enables high peptide identification rates, individualized ppb-range mass accuracies and proteome-wide protein quantification. *Nat. Biotechnol.*, **26**, 1367–1372.

Emmert-Streib,F. and Glazko,G. (2011) Pathway analysis of expression data: deciphering functional building blocks of complex diseases. *PLoS Comput. Biol.*, **7**, e1002053.

Engelman,J. *et al.* (2006) The evolution of phosphatidylinositol 3-kinases as regulators of growth and metabolism. *Nat. Rev. Genet.*, **7**, 606–619.

Goeman,J. and Bühlmann,P. (2007) Analyzing gene expression data in terms of gene sets: methodological issues. *Bioinformatics*, **23**, 980–987.

Huang,D. *et al.* (2009) Bioinformatics enrichment tools: paths toward the comprehensive functional analysis of large gene lists. *Nucleic Acids Res.*, **37**, 1–13.

Irizarry,R. *et al.* (2009) Gene set enrichment analysis made simple. *Stat. Methods Med. Res.*, **18**, 565–575.

Khatri,P. and Drăghici,S. (2005) Ontological analysis of gene expression data: current tools, limitations, and open problems. *Bioinformatics*, **21**, 3587–3595.

Klebanov,L. *et al.* (2007) A multivariate extension of the gene set enrichment analysis. *J. Bioinform. Comput. Biol.*, **5**, 1139–1153.

Kong,S. *et al.* (2006) A multivariate approach for integrating genome-wide expression data and biological knowledge. *Bioinformatics*, **22**, 2373–2380.

Li,J. and Tseng,G. (2011) An adaptively weighted statistic for detecting differential gene expression when combining multiple transcriptomic studies. *Ann. Appl. Stat.*, **5**, 994–1019.

Manning,B. and Cantley,L. (2007) Akt/pkb signaling: navigating downstream. *Cell*, **129**, 1261.

Mootha,V. *et al.* (2003) Pgc-1α-responsive genes involved in oxidative phosphorylation are coordinately downregulated in human diabetes. *Nat. Genet.*, **34**, 267–273.

Nam,D. and Kim,S. (2008) Gene-set approach for expression pattern analysis. *Brief. Bioinform.*, **9**, 189–197.

Nanjundan,M. and Possmayer,F. (2001) Pulmonary lipid phosphate phosphohydrolase in plasma membrane signalling platforms. *Biochem. J.*, **358** (Pt. 3), 637.

Ng,Y. *et al.* (2008) Rapid activation of akt2 is sufficient to stimulate glut4 translocation in 3t3-l1 adipocytes. *Cell Metabol.*, **7**, 348–356.

Ong,S. and Mann,M. (2005) Mass spectrometry–based proteomics turns quantitative. *Nat. Chem. Biol.*, **1**, 252–262.

Ong,S. *et al.* (2002) Stable isotope labeling by amino acids in cell culture, silac, as a simple and accurate approach to expression proteomics. *Mol. Cell. Proteomics*, **1**, 376–386.

Pearson,E. (1938) The probability integral transformation for testing goodness of fit and combining independent tests of significance. *Biometrika*, **30**, 134–148.

Pearson,K. (1934) On a new method of determining ''goodness of fit''. *Biometrika*, **26**, 425–442.

Perera,H. *et al.* (2003) Syntaxin 6 regulates glut4 trafficking in 3t3-l1 adipocytes. *Mol. Biol. Cell*, **14**, 2946–2958.

Poisson,L. *et al.* (2011) Integrative set enrichment testing for multiple omics platforms. *BMC Bioinformatics*, **12**, 459.

Prior,M. *et al.* (2011) Quantitative proteomic analysis of the adipocyte plasma membrane. *J. Proteome Res.*, **10**, 4970–4982.

Rivals,I. *et al.* (2007) Enrichment or depletion of a go category within a class of genes: which test? *Bioinformatics*, **23**, 401–407.

Shen,K. and Tseng,G. (2010) Meta-analysis for pathway enrichment analysis when combining multiple genomic studies. *Bioinformatics*, **26**, 1316–1323.

Stouffer,S. *et al.* (1949) *The American Soldier: Adjustment During Army Life. (Studies in Social Psychology in World War II, Vol. 1.)*, 1st edn. Princeton University Press.

Subramanian,A. *et al.* (2005) Gene set enrichment analysis: a knowledge-based approach for interpreting genome-wide expression profiles. *Proc. Natl Acad. Sci. USA*, **102**, 15545–15550.

Tan,S. *et al.* (2011) Next-generation akt inhibitors provide greater specificity: effects on glucose metabolism in adipocytes. *Biochem. J.*, **435**, 539–544.

Tseng,G.C. *et al.* (2012) Comprehensive literature review and statistical considerations for microarray meta-analysis. *Nucleic Acids Res.*, **40**, 3785–3799.

Väremo,L. *et al.* (2013) Enriching the gene set analysis of genome-wide data by incorporating directionality of gene expression and combining statistical hypotheses and methods. *Nucleic Acids Res.*, **41**, 4378–4391.

Zhao,P. *et al.* (2009) Variations in the requirement for v-snares in glut4 trafficking in adipocytes. *J. Cell Sci.*, **122**, 3472–3480.

# **Supplementary:** Direction pathway analysis of large-scale proteomics data reveals novel features of the insulin action pathway

Pengyi Yang[1,2,3*], Ellis Patrick[2*], Shi-Xiong Tan[3,4]
Daniel J. Fazakerley[3], James Burchfield[3], Christopher Gribben[3]
Matthew J. Prior[3], David E. James[3], Yee Hwa Yang[2†]

[1]Systems Biology Group, Biostatistics Branch
National Institute of Environmental Health Sciences
National Institute of Health, Research Triangle Park, NC 27709, USA

[2]School of Mathematics and Statistics, University of Sydney, NSW 2006, Australia

[3]Diabetes and Obesity Program, Garvan Institute of Medical Research, NSW 2006, Australia

[4]Metabolism in Human Disease Unit, Institute of Molecular and Cellular Biology
A*Star, 61 Biopolis Drive, Proteos 138673, Singapore

## 1 *p*-value combination

There are many methodologies for combining information across studies or within pathways and the key discriminating differences between many of these methods are their assumed alternative hypotheses (Tseng *et al.*, 2012). Let $\tau_j$ represent test statistics for $j = 1, 2, ..., n$, where $n$ are the number of tests. Assume the null hypothesis that none of the features measured by these test statistics have changed. Li and Tseng (2011) propose two broad classes of alternative hypotheses $H_A$ and $H_B$. The first class of alternative hypothesis, $H_A$, is used to detect a series of tests in which *all* the test statistics show change. The corresponding test can be expressed as

$$\begin{cases} H_0: & \tau_j = 0 \ \forall \ j = 1, 2, ..., n. \\ H_A: & \tau_j > 0 \ \forall \ j = 1, 2, ..., n. \end{cases} \tag{1}$$

The second class of alternative hypothesis, $H_B$, is used to detect a series of tests in which *any* of the test statistics show change. The corresponding test can be expressed as

$$\begin{cases} H_0: & \tau_j = 0 \ \forall \ j = 1, 2, ..., n. \\ H_B: & \tau_j > 0 \text{ for at least one } j \text{ in } 1, 2, ..., n. \end{cases} \tag{2}$$

*These authors contributed equally.
†To whom correspondence should be addressed.

Here we consider four methods of $p$-value combination that could be used to perform the previously described tests:
**Fisher:** Fisher's method is defined as $\mathrm{P}\left(\chi^2_{2n} > -2\sum_{j=1}^{n}\log(p_j)\right)$ (Fisher, 1932).
**Stouffer:** Stouffer's method is defined as $\Phi\left(\frac{\sum_{j=1}^{n}\Phi^{-1}(p_j)}{n}\right)$ (Stouffer *et al.*, 1949).
**maxP:** The maximum of the $p_j$ for $j = 1, 2, ..., n$ (Wilkinson, 1951).
**OSP:** A one-sided version of Pearson's method $\mathrm{P}\left(\chi^2_{2n} < -2\sum_{j=1}^{n}\log(1-p_j)\right)$ (Pearson, 1934).

The combined $p$-values for Fisher's and Stouffer's methods converge to zero if any one of the $p_j$ also converges to zero making them appropriate for testing $H_0$ against the alternative $H_B$. For maxP or OSP to converge to zero all $p_j$ must converge to zero, thus making them appropriate for testing $H_0$ against the alternative $H_A$. For our direction pathway analysis we would like to identify pathways that have had any of their proteins changed in all perturbations in the direction of interest. When put in the context of the two classes of alternative hypotheses, this would then require the tandem use of combination methods that favourable to testing $H_0$ against $H_A$ when combining across experimental perturbations and $H_0$ against $H_B$ when combining within a pathway, respectively.

The properties of the four methods are further illustrated in Figure 1 from a two dimensional perspective. While the arbitrary cut-offs of maxP and OSP are quite different their overall topologies are quite similar. Fisher is also seen to be quite sensitive to any change. If one of the $z$-scores is larger than approximately 2.4, then regardless of the sign of the other $z$-score, the combined $p$-value will be less than 0.05.

### 1.1 Simulation

To illustrate and distinguish the performance of the four $p$-value combination methods in relationship to the two classes of alternative hypotheses ($H_A$ and $H_B$), we perform a simulation study to assess how each method combines information from three test statistics. The distributions of the three test statistics were chosen to describe situations of no change, mild change and strong change in none, some or all of the statistics. In our simulation study, we simulate directly from the standard normal distribution, this is equivalent to simulating test statistics (potentially from a two-sample $t$-test) and transforming them into $z$-scores. In practice, these test statistics have most likely come from multiple two-sample $t$-tests but could be other statistics such as regression coefficients.

In each simulation we generated $1,000,000$ observations of the three test statistics from the multivariate normal distribution $\mathbf{X}_i \sim \mathrm{N}(\mu_i, I)$ where $\mu_1 = (0, 0, 0)$. We call this simulation I and it represents the initial test results obtained from 3 different sets of experiments. With all 3 components of $\mu_1$ equal zero, this represents the situation where test statistics were generated from comparisons with no change. We have also examine different values of $\mu$ in different simulations.

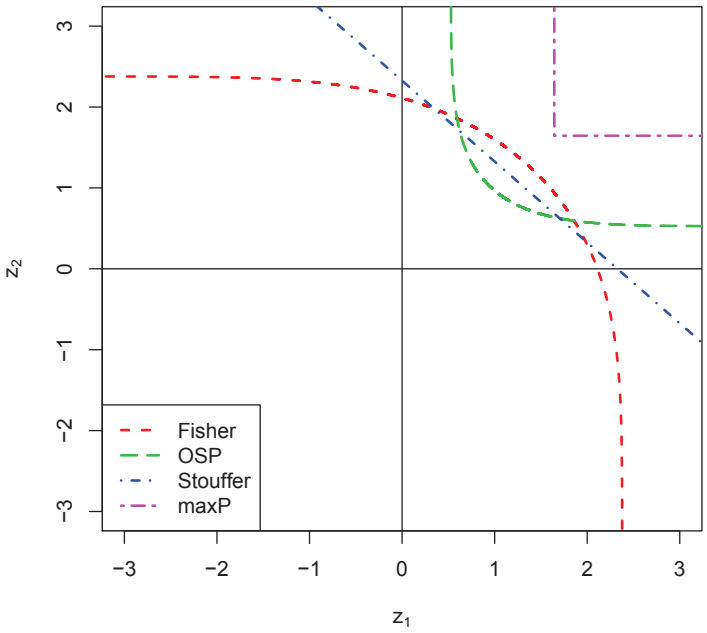


Figure 1: ***p*-value cut-offs for various combination methods** – A plot illustrating a $p$-value cut-off of 0.05 for various $p$-value combination methods in a two dimensional setting. The $p$-value cut-off is plotted in the negative $z$-score space so that a small $p$-value corresponds to a large positive $z$-score. The combination methods under consideration are Fisher (red), Stouffer (blue), maxP (pink) and OSP (green).

- $\mu_2 = (2, 0, 0)$ in simulation II ;
- $\mu_3 = (2, 2, 0)$ in simulation III;
- $\mu_4 = (4, 0, 0)$ in simulation IV and
- $\mu_5 = (2, 2, 2)$ in simulation V.

Notice, that simulation V represents the situation where all three test statistics were generated from comparisons with change. Simulations II, III and IV represent situations where at least one of the three statistics were generated from comparisons with change.

We then applied each $p$-value combination method to each observation in each simulation. An observation was called significant if its overall significance (combined $p$-value) was less than an arbitrary cut-off of 0.05. The percentage of called significance from all observations was used to characterise each method's power in performing hypothesis testing under the two classes of alternative hypotheses $H_A$ and $H_B$.

In general a method with a low percentage of significance in simulation I (as this simulation is consistent with the null hypothesis of no change) and high percentage in simulations II, III, IV and V (as these are simulations representing some change) would be a good method for testing $H_0$ against $H_B$; that an observation is changed in *any* tests. While a method with a low percentage of significance in simulations I, II, III and IV (as these are simulations where not all statistics have changed) but high percentage in simulation V (a simulation where all the statistics have changed) would be more suitable for testing $H_0$ against $H_A$; that an observation is changed in *all* tests.

### 1.2 Simulation results

Results from the simulation study can be seen in Table 1. Focusing on the results from simulation I, Fisher, Stouffer and OSP all call five percent of the observations significant. As this simulation represents the situation where test statistics were generated from comparisons with no change, all the observations called significant are false positives. As an arbitrary cut-off of 0.05 was used, it is comforting to see that the false positive rates of Fisher, Stouffer and OSP are consistent with this. Furthermore, OSP is similar with Fisher and Stouffer in simulation V but calls much less significance in simulation II, III and IV compared to the other two methods. Together, these results demonstrate that OSP is the most suitable method at testing $H_0$ against $H_A$; that an observation is changed in *all* tests.

When considering the class of alternative hypothesis $H_B$, Stouffer is most powerful in detecting observations that have changed in all three tests (simulation V). It also has higher power in detecting changes from simulations II, III, and IV when compared to OSP. In comparison, Fisher has the highest percentage in simulations II, III and IV. These results suggest that both Stouffer and Fisher are most suitable for testing $H_0$ against $H_B$ however while Fisher appears to be more sensitive to any changes, having the highest percentage in simulations II, III and IV, Stouffer is relatively more conservative.

Table 1: Results for five simulations in evaluating the performance of the four $p$-value combination methods in relationship to the two classes of alternative hypotheses $H_A$ and $H_B$. The percentage of combined $p$-values less than 0.05 over 1,000,000 simulations (rounded to two decimal places) are reported.

| Simulation | I | II | III | IV | V |
|---|---|---|---|---|---|
| methods | $\mu_1 = (0, 0, 0)$ | $\mu_2 = (2, 0, 0)$ | $\mu_3 = (2, 2, 0)$ | $\mu_4 = (4, 0, 0)$ | $\mu_5 = (2, 2, 2)$ |
| Fisher | 0.05 | 0.43 | 0.80 | 0.95 | 0.95 |
| Stouffer | 0.05 | 0.31 | 0.75 | 0.75 | 0.97 |
| maxP | 0.00 | 0.00 | 0.02 | 0.00 | 0.26 |
| OSP | 0.05 | 0.17 | 0.46 | 0.20 | 0.93 |

In our application, we select Stouffer to combine protein statistics within a pathway so that any pathway results are less likely to be driven by a single protein. These simulations demonstrate the importance of having a clearly defined alternative hypothesis in mind when analysing data.

# 2 Extended experimental procedures

3T3-L1 fibroblasts obtained from the Howard Green Laboratory (Boston, MA) were cultured in Dulbecco's modified Eagle's medium (DMEM). Fibroblasts were differentiated to adipocytes after confluent, followed by 3 days of post differentiation in growth media plus insulin (0.35 $\mu$M). Adipocytes were used between 10 to 20 passages of post-differentiation.

## 2.1 Proteomic profiling

In the two sets of mass spectrometry experiments, lysates of the cells were mixed in a 1:1:1 ratio, respectively, for each experiment. Plasma membranes from the first set were purified from cell lysates using the cationic silica isolation method described (Chaney and Jacobson, 1983). Purified PM fraction were resolved by SDS-PAGE, extracted, and digested by trypin. After tryptic digestion, peptides were separated on a Dionex Ultimate 300 LC system, and analysed by a LTQ-FT Ultra mass spectrometer. For the second set of proteomic profiling, purified PM fraction were tryptic digested and the digested peptides were subjected to strong anion exchange fractionation (SAX) on SAX-Stagetips generated in-house and analysed on an Orbitrap Velos mass spectrometer (Thermo Fisher Scientific).

Collected spectra data were preprocessed using MaxQuant software version 1.2.0.18 with the mouse IPI database v3.85. False discovery rate (FDR) at both peptide and protein group level were controlled at 1%. Only proteins that were observed within all conditions were analysed. Each sample was normalised such that the median protein

expression of that sample was zero. Two sample $t$-tests were performed for each protein in each condition with the exception of the MK samples. As there was no replication in the MK experiment, $z$-scores were calculated by assuming the variance of all the proteins were equal and was equal to the average variance of the other experiment conditions.

## 2.2 Immunoblotting

Polyclonal rabbit antibodies raised against pThr308 Akt and pSer246 PRAS40 were purchased from Cell Signaling Technologies (Beverly, MA). Polyclonal rabbit antibody raised against 14-3-3 was purchased from Santa Cruz Biotechnology, Inc. (Santa Cruz, CA). Syntaxin 6 antibody were a kind gift from Robert Piper (University of Iowa, Iowa). Rabbit polyclonal antibodies against Thr642 AS160 were as previously described (Tellam *et al.*, 1997). Horseradish peroxidase-conjugated secondary antibodies were from Amersham Biosciences (Buckinghamshire, UK) and IR dye 700 or 800 conjugated secondary antibodies were from Rockland Immunochemicals (Gilbertsville, PA). Dulbecco's modified Eagle's medium (DMEM) and F-12 medium were from Invitrogen. Fetal calf serum was from Trace Scientific (Melbourne, Australia. Bovine serum albumin (BSA) was from Bovogen (Essendon, Australia). Bicinchoninic acid reagent and SuperSignal West Pico chemiluminescent substrate were from Pierce (Rockford, IL). Protease inhibitor mixture tablets were from Roche Applied Science (Indianapolis, IN). The Akt inhibitor, MK-2206, was generously provided by Professor Dario Alessi (University of Dundee, Dundee, UK). Other materials were obtained from Sigma chemical Co (St Louis, MO).

Cells were washed twice with ice-cold PBS and solubilized in 2% SDS in PBS containing phosphatase inhibitors (1 mM sodium pyrophosphate, 2 mM sodium vanadate, 10 mM sodium fluoride) and complete protease inhibitor mixture. Insoluble material was removed by centrifugation at 18,000g for 10 min. Protein concentration was measured using the bicinchoninic acid method. Proteins were separated by SDS-PAGE for immunoblot analysis. After transferring proteins to polyvinylidene difluoride membranes, membranes were incubated in blocking buffer containing 5% skim milk in Tris-buffered saline and immunoblotted with the relevant antibodies overnight at 4 °C in blocking buffer containing 5% BSA, 0.1% Tween in Tris-buffered saline. After incubation, membranes were washed and incubated with horseradish peroxidase-labeled secondary antibodies and then detected by SuperSignal West Pico chemiluminescent substrate. Quantification of protein levels was performed using ImageJ software (Abràmoff *et al.*, 2004).

## 2.3 Live cell microscopy

42mm and 10mm Glass coverslips (PeCon GmbH, Erbach, Germany) were incubated at room temperature for 120 min with a 1:50 dilution of Matrigel in ice cold PBS. Coverslips were washed twice with PBS prior to use. After 7-9 days post-differentiation, adipocytes were trypsinised with 5x Trypsin/EDTA for 5-10 min at 37 °C, washed twice with PBS and resuspended in Electroporation Solution (20mM Hepes, 135mM KCl, 2mM MgCl2, 0.5% Ficol 400, 1% DMSO, 2 mM ATP and 5 mM Glutathione, pH7.6) along with 5-20$\mu$g of plasmid DNA. Cells were electroporated at 200mV for 20ms using an ECM 830 Square

Wave Electroporation System, (BTX Molecular Delivery Systems, Massachusetts, USA) and seeded onto matrigel coated coverslips. Adipocytes were maintained in DMEM supplemented with 10% FCS until required.

Coverslips were then mounted in a perfusion open/closed chamber (POC; PeCon GmbH, Erbach, Germany) containing modified KRP buffer (120 mM NaCl, 0.6 mM Na2HPO4, 0.4 mM NaH2PO4, 6 mM KCl, 1.2 mM MgSO4, 12.5 mM HEPES, 1 mM CaCl2, 10mM Glucose, 1x MEM Amino Acids Solution, 20 mM GlutaMAX, 0.2% (w/v) BSA, pH7.4) and placed in a heated stage microscope insert 'P' (PeCon GmbH; Erbach, Germany) on an Axiovert 200M (Carl Zeiss Microscopy GmbH, Germany) equipped with a large incubator XL (PeCon GmbH, Erbach, Germany) maintained at 37 $^{o}$C.

Healthy, suitably transfected cells were identified by brightfield and fluorescence using an appropriate objective (Typically a Zeiss A-Plan 20x/0.45). TdTomato and pHluorin were simultaneously excited using a 488/5nm bandpass filter. Emitted fluorescence was filtered by a 500nm LP filter and then split (568nm dichroic with 525/25nm and 607/70nm bandpass filters) onto two halves of an iXon DU-888D EMCCD camera (Andor, Belfast, N. Ireland) using a custom configured optosplit II (Cairn Research, Kent, UK). In this configuration, bleed through from green:red was measured at less than 3% and as such was considered negligible. All images were acquired using $\mu$Manager (Edelstein *et al.*, 2010) and analyzed using ImageJ (Abràmoff *et al.*, 2004) and Cell Profiler 2.0 (Carpenter *et al.*, 2006).

# References


Abràmoff, M. D., Magalhães, P. J., and Ram, S. J. (2004). Image processing with imagej. *Biophotonics International*, **11**(7), 36–42.

Carpenter, A. E., Jones, T. R., Lamprecht, M. R., Clarke, C., Kang, I. H., Friman, O., Guertin, D. A., Chang, J. H., Lindquist, R. A., Moffat, J., *et al.* (2006). Cellprofiler: image analysis software for identifying and quantifying cell phenotypes. *Genome Biology*, **7**(10), R100.

Chaney, L. K. and Jacobson, B. S. (1983). Coating cells with colloidal silica for high yield isolation of plasma membrane sheets and identification of transmembrane proteins. *Journal of Biological Chemistry*, **258**(16), 10062–10072.

Edelstein, A., Amodaj, N., Hoover, K., Vale, R., and Stuurman, N. (2010). Computer control of microscopes using $\mu$manager. *Current Protocols in Molecular Biology*, pages 14–20.

Fisher, R. (1932). Statistical methods for research workers.

Li, J. and Tseng, G. (2011). An adaptively weighted statistic for detecting differential gene expression when combining multiple transcriptomic studies. *The Annals of Applied Statistics*, **5**(2A), 994–1019.

Pearson, K. (1934). On a new method of determining "goodness of fit". *Biometrika*, **26**(4), 425–442.

Stouffer, S., Suchman, E., DeVinney, L., Star, S., and Williams Jr, R. (1949). The american soldier: adjustment during army life.(studies in social psychology in world war ii, vol. 1.).

Tellam, J. T., Macaulay, S. L., McIntosh, S., Hewish, D. R., Ward, C. W., and James, D. E. (1997). Characterization of munc-18c and syntaxin-4 in 3t3-l1 adipocytes putative role in insulin-dependent movement of glut-4. *Journal of Biological Chemistry*, **272**(10), 6179–6186.

Tseng, G. C., Ghosh, D., and Feingold, E. (2012). Comprehensive literature review and statistical considerations for microarray meta-analysis. *Nucleic Acids Res*, **40**(9), 3785–3799.

Wilkinson, B. (1951). A statistical consideration in psychological research. *Psychol Bull*, **48**(3), 156–158.